Eur. Phys. J. C 49, 61–64 (2007)
DOI 10.1140/epjc/s10052-006-0123-4

THE EUROPEAN PHYSICAL JOURNAL C

Regular Article – Experimental Physics

Jet properties from two-particle azimuthal correlations in $d+$Au collisions at $\sqrt{s_{NN}} = 200\,\mathrm{GeV}$ at STAR

F. Benedosso[a] for the STAR collaboration

Utrecht University, Utrecht, The Netherlands

Received: 15 August 2006 /
Published online: 2 December 2006 –

Abstract. We present measurements of azimuthal correlations between photons (from π^0 decay) and charged hadrons in $d+$Au collisions at $\sqrt{s_{NN}} = 200\,\mathrm{GeV}$. We use di-hadron correlations to study parton fragmentation in $d+$Au collisions at RHIC. Specifically, the near-side and away-side peaks of the azimuthal angular difference distribution are used to measure the root-mean-squared (RMS) fragmentation transverse momentum $\sqrt{\langle j_{\mathrm{T}}^2 \rangle}$ and the mean intrinsic parton transverse momentum $\langle |k_{\mathrm{T}_y}| \rangle$. The measurements with leading photons are compared to results using leading charged particles.

PACS. 25.75.-q

1 Introduction

In nuclear collisions at the maximum RHIC energy of $\sqrt{s_{NN}} = 200\,\mathrm{GeV}$, most of the produced particles at high-p_{T} are expected to originate from hard scattering processes. Hard scatterings of partons in the initial state produce pairs of high-p_{T} partons that fragment while traversing the medium. This fragmentation generates clusters of particles called *jets*. The structure of a jet can be modified by the hot and dense medium created in the heavy-ion collision, resulting in a softer fragmentation function or even the complete absorption of the parton [1–3]. Evidence for this has been seen both in the suppression of particle spectra at large p_{T} in central Au + Au collisions compared to $p+p$ collisions [4, 5] and in the suppression of the away side jet in central Au + Au collisions [6].

In low-multiplicity collisions, such as p+p and $d+$Au, event-by-event topological reconstruction of jets can be used to study jet production and fragmentation [7]. This approach however is not feasible in high-multiplicity Au + Au collisions and instead di-hadron azimuthal correlations of high-p_{T} particles are used. Such correlation measurements have been shown to reveal a clear di-jet structure in Au + Au collisions [5, 6, 8]. Experimentally, the two jets are not perfectly back-to-back. This effect is thought to be due to intrinsic transverse momentum of the colliding partons. At ISR energies, the mean intrinsic transverse momentum k_{T} was found to be approximately $1\,\mathrm{GeV/c}$ [9].

To characterize the jet properties we use two parameters: the transverse momentum (j_{T}) of a particle with respect to the jet axis and the transverse momentum (k_{T}) of the parton that enters the hard scattering process.

Correlation measurements are a powerful tool to study di-jet structures in $p+p$, $p+A$ and $A+A$ collisions. Properties of di-jets can be studied by measuring the yield and width of the correlation peaks. From these observables it is possible to extract j_{T} and k_{T}, and thus provide a more complete insight into the fragmentation function and the partonic intrinsic momenta.

2 Experiment and data

STAR [10] is a large acceptance detector at RHIC, dedicated to the study of the properties of the quark gluon plasma. The detector is composed of several sub-systems placed inside a large solenoidal magnet. The main detector components used for this analysis are the barrel electromagnetic calorimeter (BEMC) and the time projection chamber (TPC).

The BEMC [11] is a lead-scintillator sampling calorimeter that consists of 21 radiation lengths of material and has an energy resolution of $\Delta E/E \sim 16\%/\sqrt{E(\mathrm{GeV})}$. It has a radius of 2.3 m and a full azimuthal coverage in the pseudorapidity range $-1 < \eta < 1$. For the present analysis, only one half of the detector was operational ($0 < \eta < 1$). The calorimeter consists of 120 modules, each of them divided into 40 projective towers. Each tower has transverse dimensions of approximately $(10 \times 10)\,\mathrm{cm}^2$ which correspond to an interval $(\Delta\eta, \Delta\phi) = (0.05, 0.05\,\mathrm{rad})$ in pseudorapidity and azimuth. The towers were calibrated using minimum-ionizing particles and electrons.

[a] e-mail: benedos@phys.uu.nl

The TPC [12] also has full azimuthal coverage in the pseudo-rapidity range $|\eta| < 1$. The TPC provides up to 45 independent spatial and specific ionization $\mathrm{d}E/\mathrm{d}x$ measurements of tracks within the acceptance. The momentum resolution is $\Delta k/k \simeq 0.0078 + 0.0098 p_{\mathrm{T}}$ (GeV/c) [12], where k is the track curvature, proportional to $1/p_{\mathrm{T}}$.

The minimum bias trigger required at least one neutron in the zero degree calorimeter (ZDC) in the gold beam direction. For this analysis, a special sample of events is selected with an on-line trigger arrangement where at least one BEMC tower is above predefined threshold. Two different on-line thresholds were used the highest threshold was set at nominal $E_{\mathrm{T}} > 4.5\,\mathrm{GeV}$ and the lower threshold at 2.5 GeV. The highest threshold was chosen such that all events satisfying the trigger requirement could be recorded, while for the lower threshold a fraction of events was randomly sampled.

3 Analysis

The first step in calculating a two-particle azimuthal correlation, is to select a *leading (trigger) particle*. For each event the most energetic tower is selected as leading particle; clusters are made around the highest tower, including a maximum of 4 neighboring towers. The transverse energy E_{T} of the cluster must be included in the selected energy bin, $E_{\mathrm{T}}^{\mathrm{min}} < E_{\mathrm{T}}^{\mathrm{trigger}} < E_{\mathrm{T}}^{\mathrm{max}}$. If the most energetic tower does not satisfy this condition, the event is rejected. In the case of charged di-hadron correlation, all the tracks are considered potential trigger. Tracks with transverse momentum greater than a selected threshold but smaller than trigger energy ($p_{\mathrm{T}}^{\mathrm{threshold}} < p_{\mathrm{T}}^{\mathrm{associated}} < E_{\mathrm{T}}^{\mathrm{trigger}}$) are used as *associated tracks*. Several p_{T} (E_{T}) cuts have been used both for the trigger and the associated particles.

The azimuthal distribution between trigger and associated particle is defined as

$$D(\Delta\phi) = \frac{1}{N_{\mathrm{trigger}}} \frac{1}{\epsilon} \int N(\Delta\phi, \Delta\eta)\, \mathrm{d}\Delta\eta \qquad (1)$$

where $\Delta\phi = \phi^{\mathrm{trigger}} - \phi^{\mathrm{associated}}$, N_{trigger} is the number of trigger particles, and ϵ is the reconstruction efficiency of the TPC for the associated particles. For this analysis, the reconstruction efficiency is $\epsilon = 89\%$, independent of p_{T} and centrality [13].

Malfunctioning towers were tagged as bad and removed from the analysis. To remove contributions from charged particles in the trigger sample, all charged tracks in the events were extrapolated to the calorimeter surface and the event was rejected if one of the extrapolated tracks hits the trigger tower. A GEANT simulation [14] shows that, after applying this cut, in the selected E_{T} range the number of triggers caused by charged particles is less than 1%. A non-uniformity of the BEMC can produce systematic errors. To avoid that, towers which give too many trigger compared to the average are tagged as *hot tower* and then eliminated.

The remaining sample of trigger towers is dominated by signals from π^0 decay photons in the relevant energy range. For $E_{\mathrm{T}}^{\mathrm{trigger}} > 4.5\,\mathrm{GeV}$ the opening angle between the two photons is small, so almost all the energy of the initial particle is collected by the highest tower or cluster of tower. Simulations show that from 87% to 93% of the π^0 energy is collected, and this inefficiency has been taken into acount in the further results. A similar analysis method was used in an ISR experiment [15].

The following criteria were used to select the TPC tracks: (i) at least 25 points are used to fit the track, (ii) the distance of closest approach to the vertex along beam direction is smaller than 1 cm and (iii) the track is in the range $-1 < \eta < 1$.

4 Results

The raw correlation distribution, corrected for the efficiency and divided by the number of trigger, is fit by two Gaussian functions plus a constant

$$D(\Delta\phi) = A_N e^{-\frac{1}{2}\left(\frac{\Delta\phi}{\sigma_{\mathrm{near}}}\right)^2} + A_F e^{-\frac{1}{2}\left(\frac{\Delta\phi-\pi}{\sigma_{\mathrm{away}}}\right)^2} + B\,, \qquad (2)$$

where the first term represents the near side peak, the second the away side peak, and the third (B) is a constant term to describe the uncorrelated background.

Figure 1 shows the azimuthal correlation function after background subtraction. Panel (a) shows the correlation function for $4.5 < E_{\mathrm{T}}^{\mathrm{trigger}} < 6.5\,\mathrm{GeV}$ and $p_{\mathrm{T}}^{\mathrm{associated}}$ greater than 2, 3 and 4 GeV/c and always smaller than $E_{\mathrm{T}}^{\mathrm{trigger}}$. In panel (b) the lower threshold for $p_{\mathrm{T}}^{\mathrm{associated}}$ is fixed at 2 GeV/c while $E_{\mathrm{T}}^{\mathrm{trigger}}$ varies in the bins 4.5–6.5 GeV, 6.5–8.5 GeV or 8.5–10.5 GeV. All errors are statistical only.

There is a significant systematic uncertainty in the vertical scale of Fig. 1. Backgrounds from upstream interactions of the beam with material in the accelerator lead to a measurable fraction of the BEMC high tower triggers [16]. A more detailed study of the systematic uncertainties due to these backgrounds is still in progress.

The correlation distribution shows the behavior expected for di-jets event, with a near side peak centered at $\Delta\phi = 0$ and an away side peak at $\Delta\phi{=}\pi$. The peak height decreases with $p_{\mathrm{T}}^{\mathrm{associated}}$ and it increases with $E_{\mathrm{T}}^{\mathrm{trigger}}$ while the widths are more sensitive to $p_{\mathrm{T}}^{\mathrm{associated}}$. The observations are in qualitative agreement with expectations from di-jet fragmentation, in which most energetic particles lie closer to the leading one, and thereby the width decreases with $p_{\mathrm{T}}^{\mathrm{associated}}$; on the other hand, higher $E_{\mathrm{T}}^{\mathrm{trigger}}$ tags more energetic jets so a greater multiplicity is expected.

The near and away-side peaks widths σ_{near} and σ_{away} as determined from a fit of the assumed correlation shape (2) to the measured distributions is shown in Fig. 2 and compared to results for charged particles. The near side peak is narrower than the away-side peak in each $E_{\mathrm{T}}^{\mathrm{trigger}}$ and $p_{\mathrm{T}}^{\mathrm{associated}}$ bin. The correlation peak widths for γ-charged hadron and charged di-hadron correlations are similar. As observed for the raw distributions, the peak width decreases with $p_{\mathrm{T}}^{\mathrm{associated}}$: high p_{T} particle are closer to leading particle. The peaks get narrower with increasing

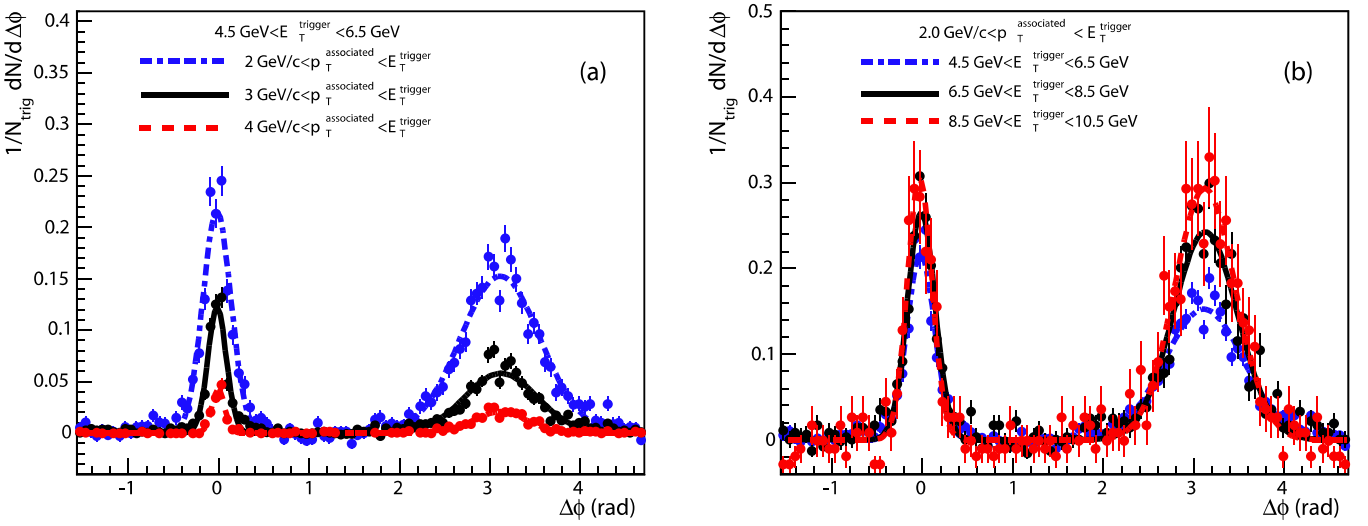

Fig. 1. Preliminary results for γ-charged correlation function after background subtraction. Panel **a** shows the correlation distribution as a function of $p_{\mathrm{T}}^{\mathrm{associated}}$; panel **b** shows the correlation as a function of $E_{\mathrm{T}}^{\mathrm{trigger}}$

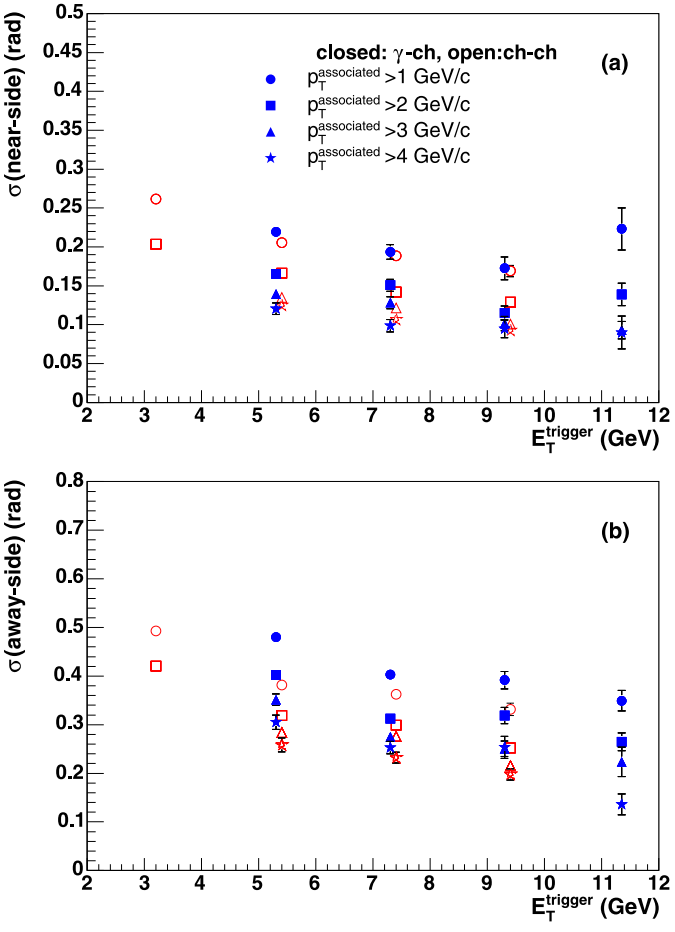

Fig. 2. Preliminary results for gaussian widths for near side **a** and away side **b** peak as function of $E_{\mathrm{T}}^{\mathrm{trigger}}$. The bins for $p_{\mathrm{T}}^{\mathrm{associated}}$ are indicated. *Open symbols* are for charged di-hadron, *close* for γ-charged. The *data points* for charged di-hadron correlations are artificially shifted by 0.1 GeV/c for a better view. Errors are statistical only. $E_{\mathrm{T}}^{\mathrm{trigger}}$ for trigger photons are plotted after correction for leakage factors

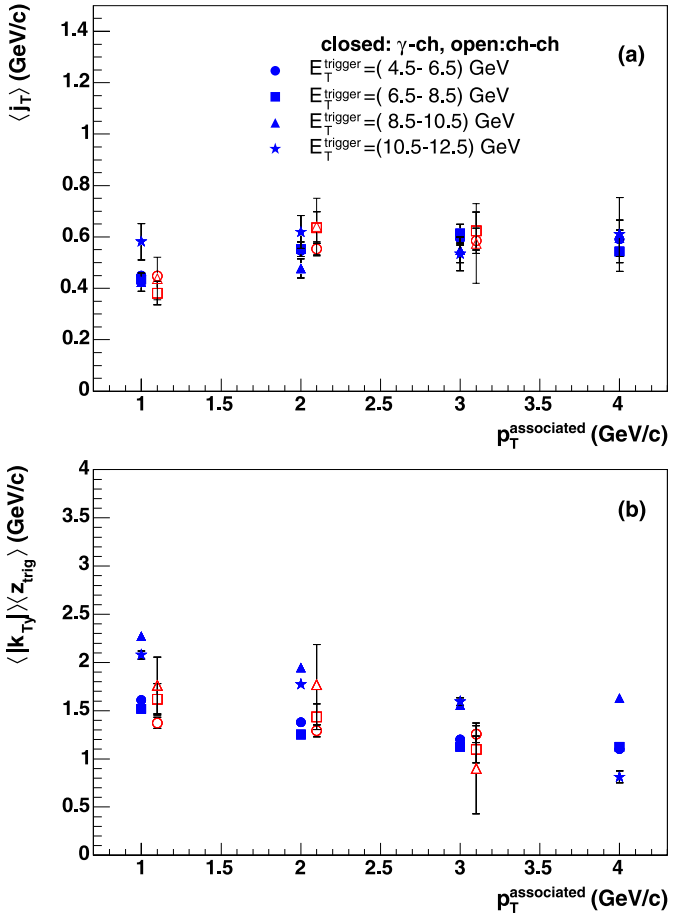

Fig. 3. **a** $\sqrt{\langle j_{\mathrm{T}}^2 \rangle}$ and **b** $\langle |k_{\mathrm{T}}| \rangle \langle z_{\mathrm{trigger}} \rangle$ for γ-charged and charged di-hadron correlations as a function of p_{T} of associated particles. The *data points* for charged di-hadron correlations are artificially shifted by 0.1 GeV/c for a better view

$E_{\mathrm{T}}^{\mathrm{trigger}}$. This is consistent with the idea of getting more energetic associated particle in the more energetic jets. Moreover, for higher-p_{T} triggers, the trigger particle is closer to the jet axis and than it narrows the trigger-associated correlation peak.

The figures show only statistical errors; the errors increase at large $E_{\mathrm{T}}^{\mathrm{trigger}}$ and $p_{\mathrm{T}}^{\mathrm{associated}}$ because of the reduced statistics.

4.1 Jet properties

To further quantify the jet shape information from the di-hadron correlation measurements, we calculated the RMS fragmentation transverse momentum using the relation [17]

$$\sqrt{\langle j_{\mathrm{T}}^2\rangle} \approx \sqrt{\frac{\pi}{2}}\sigma_{\mathrm{Near}} \frac{\langle E_{\mathrm{T}}^{\mathrm{trigger}}\rangle \langle p_{\mathrm{T}}^{\mathrm{associated}}\rangle}{\sqrt{\langle E_{\mathrm{T}}^{\mathrm{trigger}}\rangle^2 + \langle p_{\mathrm{T}}^{\mathrm{associated}}\rangle^2}} . \quad (3)$$

The effective transverse momentum of the colliding partons can also be studied with di-hadron correlations. Its average can be approximated as

$$\langle |k_{\mathrm{T}_y}|\rangle \langle z_{\mathrm{trigger}}\rangle \approx \frac{\langle z_{\mathrm{trigger}}\rangle \langle E_{\mathrm{T}}^{\mathrm{trigger}}\rangle \sqrt{\sigma_{\mathrm{Far}}^2 - \sigma_{\mathrm{Near}}^2}}{\sqrt{\pi}} . \quad (4)$$

Since $\langle z_{\mathrm{trigger}}\rangle$ is unknown, the quantity $\langle |k_{\mathrm{T}_y}|\rangle \langle z_{\mathrm{trigger}}\rangle$ is studied. In Fig. 3 $\sqrt{\langle j_{\mathrm{T}}^2\rangle}$ is shown as a function of $E_{\mathrm{T}}^{\mathrm{trigger}}$. $\sqrt{\langle j_{\mathrm{T}}^2\rangle}$ shows no significant dependence on $p_{\mathrm{T}}^{\mathrm{associated}}$, as expected. $\langle |k_{\mathrm{T}_y}|\rangle \langle z_{\mathrm{trigger}}\rangle$, however shows a slight dependence on associated $p_{\mathrm{T}}^{\mathrm{associated}}$, which could be due to a dependence of $\langle z_{\mathrm{trigger}}\rangle$ on $p_{\mathrm{T}}^{\mathrm{associated}}$. The results from charged di-hadron correlations and gamma-charged hadron correlations are in qualitative agreement. A more detailed investigation of systematic uncertainties and the energy scale corrections for gamma-charged hadron correlations is in progress.

5 Conclusion and outlook

We observed back-to-back structure of γ-charged hadron and charged di-hadron azimuthal correlation , which agrees with production of di-jet events.

It has been observed that the away side peak is always wider than the corresponding near side peak. If $E_{\mathrm{T}}^{\mathrm{trigger}}$ is fixed, when $p_{\mathrm{T}}^{\mathrm{associated}}$ increases the width of the peaks decreases, indicating that particle with larger p_{T} tend to lie closer to the leading one. The dependence on $E_{\mathrm{T}}^{\mathrm{trigger}}$ is less strong.

The values for $\sqrt{\langle j_{\mathrm{T}}^2\rangle}$ obtained from di-hadron correlations are in agreement with values obtained from full jet reconstruction [15].

Within current statistical and systematic uncertainties, no differences between di-hadron correlations with lead π^0 and leading charged particles are seen. Assuming that the leading charged particles are dominantly pions, this is consistent with the expected isospin symmetry.

Parallel analysis on $p+p$ data will give a more complete description of the system and a solid reference for further Au$+$Au analysis.

References

1. M. Gyulassy, M. Plumer, Phys. Lett. B **243**, 432 (1990)
2. X.N. Wang, M. Gyulassy, Phys. Rev. Lett. **68**, 1480 (1992)
3. R. Baier, D. Schiff, B.G. Zakharov, Ann. Rev. Nucl. Part. Sci. **50**, 37 (2000)
4. PHOENIX Collaboration, K. Adcox et al., Phys. Rev. Lett. **88**, 022 301 (2002)
5. STAR Collaboration, C. Adler et al., Phys. Rev. Lett. **90**, 082302 (2003)
6. STAR Collaboration, J. Adams et al., Phys. Rev. Lett. **91**, 072 304 (2003)
7. STAR Collaboration, T. Henry, J. Phys. G **30**, S1287 (2004)
8. STAR Collaboration, D. Magestro, in: Quark Matter 2005, 18th Int. Conf. Nucleus–Nucleus Interactions, August 4–9, 2005, Budapest, Hungary
9. M. Della Negra et al., Nucl. Phys. B **127**, 1 (1977)
10. STAR Collaboration, K.H. Ackermann et al., Nucl. Instrum. Methods Phys. Res. **499**, 624 (2003)
11. M. Beddo et al., Nucl. Instrum. Methods Phys. Res. **499**, 725 (2003)
12. M. Anderson et al., Nucl. Instrum. Methods Phys. Res. **499**, 659 (2003)
13. STAR Collaboration, C. Adler et al., Phys. Rev. Lett. **87**, 112 303 (2001)
14. P. Nevski, in: Proc. Int. Conf. Computating in High Energy and Nuclear Physics, Padova, Italy, 2000
15. CCOR, A.L.S. Angelis et al., Phys. Lett. B **97**, 163 (1980)
16. STAR Collaboration, M.J. Russcher, these proceedings
17. PHENIX Collaboration, S.S. Adler et al., Phys. Rev. C **73**, 054 903 (2006)